CP1 and Tribicarb-3D: unique long-term and large-scale *in situ* migration tests in Boom Clay at the HADES Underground Research Laboratory

Marc Aertsens[1]*, Eef Weetjens[1], Joan Govaerts[1], Norbert Maes[1] and Stéphane Brassinnes[2]

[1]SCK CEN, Belgian Nuclear Research Centre, Institute for Environment, Health and Safety, Boeretang 200, B-2400 Mol, Belgium

[2]ONDRAF/NIRAS, Kunstlaan 14, B-1210 Brussels, Belgium

MA, 0000-0003-3258-6416

*Correspondence: marc.aertsens@sckcen.be

Abstract: Assessing the long-term safety of a deep geological repository for the disposal of radioactive waste depends on an adequate understanding of the processes governing radionuclide transport. From the early days of the research on geological disposal in clay in Belgium, large-scale, long-term *in situ* migration experiments were started to test whether our knowledge acquired about small-scale samples can be scaled up in time and space. These experiments use multi-filter piezometers to introduce radiotracers in a 'source filter' and monitor their breakthrough in 'monitoring filters'. The CP1 experiment started in 1988 and used HTO as a tracer, while the Tribicarb-3D started in 1995 and used a cocktail of HTO and $H^{14}CO_3^-$. At the start of these experiments, blind predictions were made based on lab-derived parameters and a simple representation of the hydrological system. Several decades later, these blind predictions still describe the data remarkably well. These tests provide valuable data for upscaling and validating the transport models in Boom Clay and allow us to estimate transport parameters at a larger scale. They provide strong arguments that the radiological safety of a deep geological repository in a clay rock can be guaranteed.

Disposal of radioactive waste in a deep geological repository is considered as a possible long-term solution for high- and intermediate-level, long-lived, radioactive waste. The basic idea is to isolate the waste in a deep geological repository where it should be contained for a very long time. Host rocks typically considered are crystalline and volcanic rocks, clay and salts. The choice of rock in a country is mainly determined by the availability of geological formations with suitable intrinsic properties and environmental conditions, at sites where the local community accepts the final disposal of the waste.

In Belgium, Boom Clay is being studied as one of the candidate host rocks. Advantages of Boom Clay are a very low water flow (Aertsens *et al.* 2004; Yu *et al.* 2013), swelling behaviour leading to a self-sealing ability (Bastiaens *et al.* 2007) and a high retention of cationic radionuclides (De Cannière *et al.* 1996; Baetsle 1998; Maes *et al.* 2011; Salah *et al.* 2013; Altmann *et al.* 2015; Bruggeman and Maes 2017). Safety assessment studies (e.g. Marivoet and Weetjens 2007) allow estimating the radiological impact of the very small residual fraction of long-lived radionuclides that may eventually be released into the biosphere. These studies require values for the transport parameters in the various components of the disposal system, of which the undisturbed Boom Clay is one of the most important.

The Boom Clay transport parameters are mainly estimated on small-scale cores (order of centimetres) in lab experiments under *in situ* relevant conditions. The Boom Clay is relatively homogeneous, apart from some heterogeneities such as septaria or the organic 'Double Band' (e.g. Vandenberghe 1978; De Craen 1998; Aertsens *et al.* 2004; De Craen 2006). However, lab results always need to be confirmed by larger-scale experiments and natural observations, for example by *in situ* experiments (Delay *et al.* 2014), or natural tracer profiles (Mazurek *et al.* 2011). In this paper, we discuss these large-scale *in situ* experiments.

In addition to the larger scale, these experiments have the advantage that they represent disposal conditions as closely as possible. *In situ* experiments in Boom Clay are performed in the HADES Underground Research Laboratory (URL). The HADES URL, whose construction started in 1980, is the oldest, first-of-a-kind, URL in clay. It is operated by the Economic Interest Grouping (EIG) Euridice, a partnership between the Belgian Nuclear Research Centre SCK CEN and the Belgian Agency for Radioactive Waste Management and Enriched Fissile

From: Li, X. L., Van Geet, M., Bruggeman, C. and De Craen, M. (eds) 2023. *Geological Disposal of Radioactive Waste in Deep Clay Formations: 40 Years of RD&D in the Belgian URL HADES.*
Geological Society, London, Special Publications, **536**, 131–144.
First published online January 11, 2023, https://doi.org/10.1144/SP536-2022-41

Materials ONDRAF/NIRAS. The HADES URL is conveniently located at a depth of 225 m below the EIG Euridice, situated next to SCK CEN. The Boom Clay thickness here is approximately 100 m. The Boom Clay mineralogy consists of 30–70% clay minerals (mainly smectite, illite and interstratified smectite/illite), 15–53% quartz and 0.1–10% plagioclase and potassium feldspar (De Craen *et al.* 2004; Zeelmaekers *et al.* 2015; Frederickx 2019; Frederickx *et al.* 2021). Boom Clay contains up to 5 wt% of natural organic matter with up to 250 mg C l^{-1} collected in pore water (De Craen *et al.* 2004; Durce *et al.* 2015).

This paper focuses on two large-scale *in situ* migration experiments in the HADES URL (Aertsens *et al.* 2013; Aertsens 2014) using unretarded/weakly retarded tracers: CP1 and Tribicarb-3D. Both experiments have been ongoing for more than three decades: CP1 (since 1988, *c.* 34 years) and Tribicarb-3D (since 1995, *c.* 27 years). Their objective is to investigate whether our understanding of the transport phenomena in the host rock is good enough and whether the transport parameters determined from lab experiments are valid for larger time and space scales. Therefore, at the start of these experiments, a blind prediction was made for the tracer concentrations at fixed positions as a function of time. These were based on diffusion parameters obtained from lab experiments at that time (Put and Henrion 1988, 1992; Henrion *et al.* 1991).

In both tests, HTO (tritiated water) is used as a tracer. HTO is a small, neutral and unretarded tracer, not subjected to electrostatic interactions. This allows it to be distributed uniformly over the entire pore space, which explains why it is used as a reference molecule for the transport parameters of a whole range of solutes. In Tribicarb-3D, an anionic tracer $H^{14}CO_3^-$ (which may show weak retention) is injected simultaneously with HTO. Anionic tracers like iodide or $H^{14}CO_3^-$ (^{14}C is an important activation product in spent fuel) diffuse relatively quickly through clay (no or negligible sorption, anion exclusion) and could pose a radiological hazard (e.g. Marivoet 1988; Marivoet and Zeevaert 1991).

All measurement points in CP1 are on a single line, while in Tribicarb-3D they are distributed in three dimensions (hence the suffix 3D in Tribicarb-3D). This allows the anisotropy of diffusion in Boom Clay to be studied more accurately than in CP1. In addition to CP1 and Tribicarb-3D, a third large-scale *in situ* test was launched in 1992: TD41HV (De Cannière *et al.* 1996; Aertsens *et al.* 2013; Aertsens 2014). This test used iodide $^{125}I^-$ as a tracer. Due to the limited half-life of $^{125}I^-$ (60 days), the concentration of the source was below the detection limit after three years and the experiment was discontinued (and is not considered further in this paper). This setup was, however, used again to study the diffusion behaviour of dissolved organic matter (DOM) colloids (using ^{14}C-labelled DOM) (Dierckx *et al.* 2000; Martens *et al.* 2010; Govaerts *et al.* 2022). In CP1 and Tribicarb-3D, tracers are used with long half-lives and they provide measurable data for many years and on a large scale making them very suitable for upscaling purposes.

Over the years, the results of these tests have been reported and compared with the blind predictions (De Preter *et al.* 1992; Put *et al.* 1991, 1993; De Cannière *et al.* 1996, 2007; Aertsens *et al.* 2013). As the understanding of modelling transport in clay layers increased and the modelling (analytical, numerical) methods and capabilities improved, these tests were also used to validate the transport models in Boom Clay (HTO data: Weetjens *et al.* 2011, 2014) and to re-estimate with these models and the experimental data the transport parameters through optimization (HTO data: Weetjens *et al.* 2011, 2014; Aertsens *et al.* 2013; HTO and $H^{14}CO_3^-$ data: Aertsens *et al.* 2013).

This paper builds on these previous works and does not intend to provide a comprehensive overview of the evolution of the modelling/interpretation of these experiments. The focus of this paper is on the inverse modelling extracting from the experiments the transport parameters relevant for large spatial scales by using analytical (MICOF) and numerical (COMSOL) modelling approaches. This inverse modelling exercise uses the latest dataset.

The CP1 and Tribicarb-3D Experiments

These large-scale *in situ* experiments use multi-filter piezometers emplaced in boreholes (Fig. 1) (Monsecour *et al.* 1990; Beaufays *et al.* 1994; Aertsens 2014). These boreholes are drilled into the clay formation from the HADES URL and flushed with inert gas to prevent significant oxidation of the clay. Then, the multi-filter piezometer – a stainless steel cylindrical tube with a series of filter screens up to 0.5 to 1 m apart – is placed into the borehole. Due to the high plasticity of the clay, the clay closes around the filters and no packer is needed to hydraulically isolate the different filter intervals.

The filters are equipped with one or two stainless steel tubes leading to the gallery and allowing the injection and withdrawal of water, or recirculation in case of two tubes. In the injection filter (often the central filter), a radiotracer solution is injected or circulated and water samples are taken at regular times from the injection filter and the adjacent filters. This enables us to establish 'breakthrough' curves of these tracers at different distances.

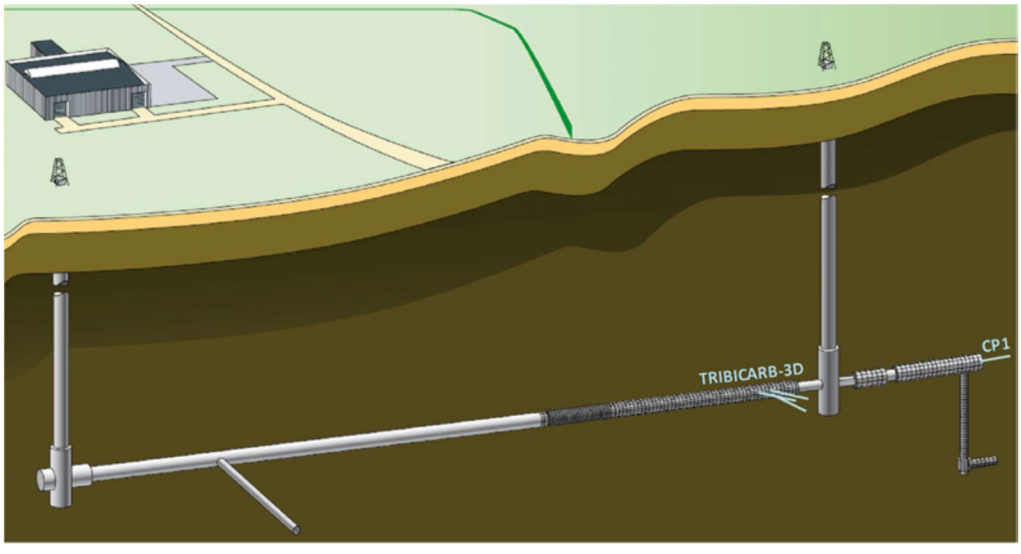

Fig. 1. Location of the *in situ* migration experiments CP1 and Tribicarb-3D at the Hades URL.

In Boom Clay, the *in situ* diffusion tests do not significantly suffer from a borehole-disturbed zone (BDZ) as the damaged clay skin around the filters is rapidly sealed by the fast convergence/creep of the plastic clay around the piezometer casing. Since there is no intention to overcore these piezometers and they will remain in place, the experiment can run over several years and the tracers can migrate over several metres without being affected by the already negligible BDZ. These tests have no end date and they continue to provide reliable data for several years or even decades. They are therefore very valuable with respect to upscaling to tens of years and up to several metres. The CP1 setup is a single horizontally placed multi-filter piezometer located behind a concrete plug (hence the name 'CP') at one end of the HADES URL (Figs 1 & 2). In 1988, HTO was injected in the central filter (filter 5). The distance between the centres of neighbouring filters is 1 m (Monsecour *et al.* 1990; Put *et al.* 1993; Beaufays *et al.* 1994; Aertsens 2014, Fig. 4). The pressure difference between the open gallery of the HADES URL (1 atm) and the *in situ* pressure (22 atm) results in water flowing towards the gallery and the tracer is transported by both diffusion and advection.

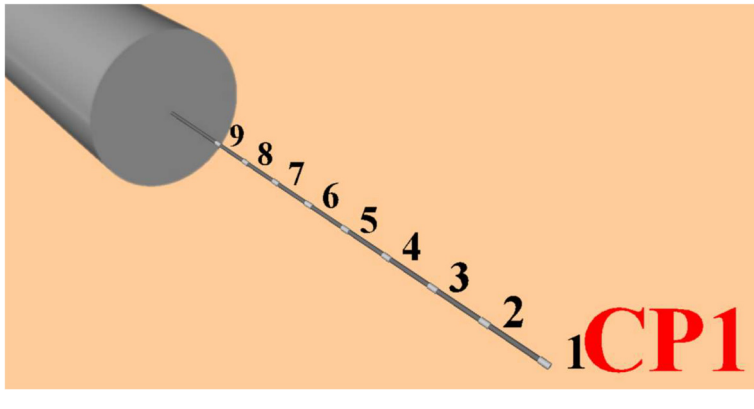

Fig. 2. Configuration of the CP1 experiment: a piezometer with filters is drilled horizontally into the Boom Clay at the end of (and parallel with) the HADES URL. The numbers indicate the filters. The distance between the centres of consecutive filters is 1 m. At zero time, the tracer (HTO) was injected in filter 5.

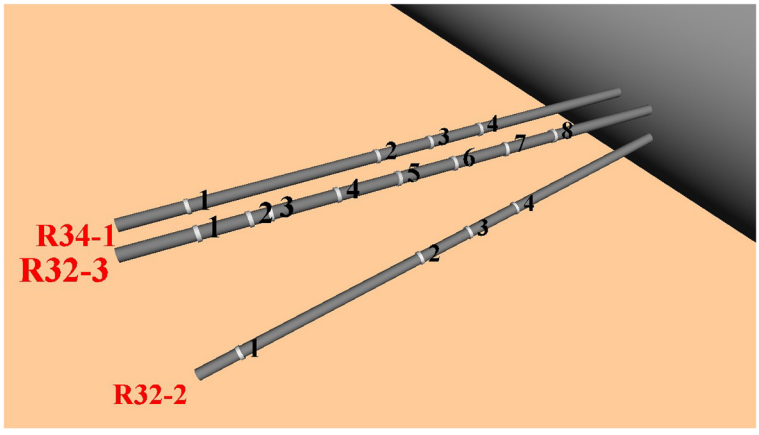

Fig. 3. Configuration of the Tribicarb-3D experiment: two horizontal, approximately parallel, piezometers (R34-1 and R32-3) and an inclined piezometer (R32-3) were drilled into the Boom Clay around the URL. The numbers indicate the filters on the piezometers. At zero time, the tracer (HTO and $H^{14}CO_3^-$) was injected in filter 6 of piezometer R32-3.

An extension of this kind of test is the emplacement of several multi-filter piezometers in a 3D configuration. This also enables the sampling in neighbouring piezometers providing 3D spatial information at a scale of metres. This principle is used in the Tribicarb-3D experiment, which is located along the gallery of the URL (Fig. 1). In the same way as in CP1, HTO (tritiated water) and $H^{14}CO_3^-$ (bicarbonate), were injected (in 1995) in a central filter on a horizontal piezometer (R32-3, Fig. 3). Nearby are two additional piezometers: one (R34-1, Fig. 3) is parallel to and approximately at the same height as R32-3, while the second piezometer (R32-2, Fig. 3) is inclined with respect to both other piezometers. The detailed filter positions are given in Table 1 and (Put 1999; Aertsens *et al.* 2013; Aertsens 2014). The water flow pattern around the cylindrical gallery (Tribicarb, Fig. 3) is slightly different from what occurs at the end of the gallery (CP1, Fig. 2).

Twice a year, water is sampled from the filters and the activity of the radiotracers (both beta emitters) is determined using liquid scintillation counting. Measurement errors for HTO are typically around 15% at

Table 1. *Filter positions in the Tribicarb-3D experiments, as well as the distance to the source (origin) and the distance to the end of the piezometer (at the URL)*

	x (m)	*y* (m)	*z* (m)	To origin (m)	To URL (m)
R32-3 Source piezometer					
R32-3-8	−1.985	−0.245	−0.024	2.00	3
R32-3-7	−0.992	−0.122	−0.012	1.00	4
R32-3-6	0.000	0.000	0.000	0.00	5
R32-3-5	0.992	0.122	0.012	1.00	6
R32-3-4	1.985	0.245	0.024	2.00	7
R32-2 Inclined piezometer					
R32-2-4	−1.192	0.014	−1.220	1.71	4
R32-2-3	−0.219	0.144	−1.410	1.43	5
R32-2-2	0.755	0.274	−1.599	1.79	6
R34-1 Parallel piezometer					
R34-1-4	−0.882	−1.009	−0.042	1.34	4
R34-1-3	0.111	−0.889	−0.044	0.90	5
R34-1-2	1.103	−0.769	−0.046	1.35	6

Only filters whose tracer concentration is not too low to measure are considered.

low tracer concentrations, decreasing to 5% at higher concentrations. For $H^{14}CO_3^-$, these errors can be higher for two reasons. First, $H^{14}CO_3^-$ is unstable and tends to escape from the clay water after transforming to the gaseous form of $^{14}CO_2$. To prevent this, the $H^{14}CO_3^-$-enriched solution sampled from the filters is collected in a background of NaOH to avoid the escape of CO_2 (Aertsens 2014). Second, the activity spectra in liquid scintillation counting of both isotopes overlap, making it difficult to distinguish both isotopes. Since the HTO activity is initially one to two orders of magnitude higher than the $H^{14}CO_3^-$ activity, the measured $H^{14}CO_3^-$ activity cannot be considered as very reliable. Details of the activity measurements are given in Aertsens *et al.* (2013) and Aertsens (2014).

Modelling

The transport of a decaying tracer through Boom Clay is assumed to be described by the advection–dispersion equation with an additional decay term:

$$\frac{\partial C}{\partial t} = \mathrm{div}((D_{\mathrm{app}} + D_{\mathrm{h}})\,\mathrm{grad}\,C + \overrightarrow{V_{\mathrm{app}}}\,C) - \lambda C \tag{1}$$

with $C(x, y, z, t)$ the tracer concentration in the clay pore water (Bq m^{-3}), (x, y, z) position (m, m, m), t time (s), D_{app} the apparent diffusion coefficient tensor (m^2 s^{-1}), D_{h} the hydrodynamic dispersion tensor (m^2 s^{-1}), $\overrightarrow{V_{\mathrm{app}}}$ the apparent velocity (m s^{-1}) and λ the decay constant (1 s^{-1}).

The advection–dispersion equation (1) is solved in two ways: (i) an analytical solution, called the MICOF model (Put and Henrion 1992); and (ii) a numerical solution with COMSOL multiphysics version 3.5a, Earth Science Module (2008). MICOF is the original model developed when CP1 was started. Since then, more general and complex numerical codes, such as COMSOL, have become available. These codes, which allow us to solve equation (1) without some of the simplifying assumptions of MICOF, have been used to model these experiments. Solving equation (1) with both codes allows their verification.

Analytical solution (MICOF model)

It is assumed that at all positions (x, y, z) the Darcy velocity $\overrightarrow{V_{\mathrm{Darcy}}}$ due to drainage towards the URL gallery is the same. The x-axis (unit vector $\overrightarrow{e_x}$) is chosen parallel to this velocity ($\overrightarrow{V_{\mathrm{Darcy}}} = V_{\mathrm{Darcy}}\,\overrightarrow{e_x}$). Both the x-axis and the y-axis are taken parallel to the bedding plane of the clay, so that the corresponding apparent diffusion coefficients are equal ($D_{\mathrm{app},x} = D_{\mathrm{app},y}$). Neglecting the transversal dispersion length, expression (1) reduces to:

$$\frac{\partial C}{\partial t} = D^i_{\mathrm{app},x}\frac{\partial^2 C}{\partial x^2} + D_{\mathrm{app},x}\frac{\partial^2 C}{\partial y^2} + D_{\mathrm{app},z}\frac{\partial^2 C}{\partial z^2} - V_{\mathrm{app}}\frac{\partial C}{\partial x} - \lambda C \tag{2}$$

with $D_{\mathrm{app},z}$ the apparent diffusion coefficient perpendicular to the bedding and $D^i_{\mathrm{app},x}$ the apparent dispersion coefficient:

$$D^i_{\mathrm{app},x} = D_{\mathrm{app},x} + \alpha\, V_{\mathrm{app}} \tag{3}$$

where α is the (longitudinal) dispersion length (m) and $V_{\mathrm{app},x}$ (m s^{-1}) the apparent velocity, which is supposed to be related to the Darcy velocity (m s^{-1}) by:

$$V_{\mathrm{app}} = \frac{V_{\mathrm{Darcy}}}{\eta R} \tag{4}$$

The rock capacity factor ηR (−) is the product of the accessible porosity η (−) and the retardation factor R. Both tracers, HTO and the $H^{14}CO_3^-$, are considered here as unretarded allowing us to put $R = 1$. We point out that expression (4) is only correct for HTO, but not for anions such as $H^{14}CO_3^-$, as discussed in Aertsens *et al.* (2020). The apparent velocity V_{app} can be fitted from experiments, but for anions, this fitted value is not the ratio V_{Darcy}/η because there is also water flow in anion inaccessible porosity (Aertsens *et al.* 2020). Using expression (4) therefore overestimates the apparent velocity $V_{\mathrm{app},x}$ for anions. In this paper, we use the standard expression (4) due to the lack of a correct expression, but it does not affect the interpretation.

For the initial blind prediction, the values of $D_{\mathrm{app},x}$, $D_{\mathrm{app},z}$, the accessible porosity η and the dispersion length α were estimated from lab experiments. The value of the Darcy velocity (m s^{-1}) was determined from:

$$V_{\mathrm{Darcy}} = K_x\frac{dh}{dx} \tag{5}$$

with K_x the hydraulic conductivity parallel to the bedding plane (m s^{-1}) and dh/dx the hydraulic head (m m^{-1}) measured between two filters.

With respect to the value for the dispersion length α, although the advection–dispersion equation is commonly used to describe advective/dispersive transport (e.g. Aertsens *et al.* 1999, 2003, 2008*a*, *b*; Chen *et al.* 2018*a*, *b*), it may not be entirely correct since according to Hunt *et al.* (2011, p. 412):

> the advection–dispersion equation is more or less universally accepted to be correct at the scale of one pore and its predictions are not borne out at any scale larger than this.

One problem of the advection–dispersion equation is the dispersion length α, whose value strongly

Table 2. *Summary of the parameter values used for the blind predictions using the MICOF model*

			HTO CP1	HTO Tribicarb-3D	$H^{14}CO_3^-$ Tribicarb-3D
Apparent diffusion coefficient	$D_{app,x}$	($m^2\ s^{-1}$)	4.10×10^{-10}	4.10×10^{-10}	1.20×10^{-10}
Apparent diffusion coefficient	$D_{app,z}$	($m^2\ s^{-1}$)	2.05×10^{-10}	2.05×10^{-10}	6.00×10^{-11}
Hydraulic head	dh/dx	(m/m)	18.9	24.1	24.1
Hydraulic conductivity	K_x	($m\ s^{-1}$)	3.2×10^{-12}	3.2×10^{-12}	3.2×10^{-12}
Darcy velocity	V_{Darcy}	($m\ s^{-1}$)	6.0×10^{-11}	7.6×10^{-11}	7.6×10^{-11}
Accessible porosity	η	(–)	0.35	0.35	0.33
Apparent velocity	$V_{app,x}$	($m\ s^{-1}$)	1.7×10^{-10}	2.18×10^{-10}	2.3×10^{-10}
Dispersion length	α	(m)	2×10^{-3}	2×10^{-3}	2×10^{-3}
Apparent dispersion coefficient	$D^i_{app,x}$	($m^2\ s^{-1}$)	4.10×10^{-10}	4.10×10^{-10}	1.20×10^{-10}
Decay constant	λ	($1\ s^{-1}$)	1.79×10^{-9}	1.79×10^{-9}	3.83×10^{-12}
Injected tracer quantity	Q_0	(Bq)	1.25×10^{9}	2.21×10^{9}	7.00×10^{8}

Put (1999), Aertsens *et al.* (2013), Aertsens (2014), expressions (3) to (5).

depends on the scale of the experiment and can vary over 10 orders of magnitude of spatial scale (Hunt *et al.* 2011; Hunt and Sahimi 2017). Table 2 clearly shows that for a dispersion length $\alpha = 2 \times 10^{-3}$ m, estimated from lab experiments (Put 1992; Aertsens *et al.* 1999) on clay cores with a length of a few centimetres and consistent with the range mentioned in Hunt *et al.* (2011) and Hunt and Sahimi (2017), the dispersive term αV_{app} in expression (3) is negligible ($D^i_{app,x} \approx D_{app,x}$). At the metre scale (relevant for these experiments), the dispersion length is still lower than 1 m according to Hunt *et al.* (2011) and Hunt and Sahimi (2017), and the dispersive term αV_{app}, in expression (3) remains negligible ($D^i_{app,x} \approx D_{app,x}$).

With the present pressure gradient in Boom Clay, due to the limited scale of the *in situ* experiments (of the order of metres) the dispersion term in expression (3) is negligible compared to diffusion (Table 2). Because expression (6) and the COMSOL numerical solution (Weetjens *et al.* 2014) both describe the experimental data well during the first 15–20 years (Aertsens *et al.* 2013; Weetjens *et al.* 2014), it is clear that the advection–dispersion equation can be used to adequately model these experiments.

Approximating the injection filter at ($x = 0$, $y = 0$, $z = 0$) as a point source, which is equivalent to assuming that the dimensions of the injection filter (8.5 cm, Put *et al.* 1993; Beaufays *et al.* 1994) are much smaller than the distances to the measuring filters (the distance between consecutive filters is 1 m), leads to the following solution (Aertsens *et al.* 2013): with Q_0 the injected tracer quantity (Bq) at $t = 0$.

$$C(x, y, z, t) = \frac{Q_0 \exp\left(-\frac{(x - V_{app}t)^2}{4D^i_{app,x}t}\right) \exp\left(-\frac{y^2}{4D_{app,x}t}\right) \exp\left(-\frac{z^2}{4D_{app,z}t}\right) \exp(-\lambda t)}{8\,\eta\sqrt{D^i_{app,x}D_{app,y}D_{app,z}t^3}} \quad (6)$$

Numerical solution (COMSOL)

The numerical modelling using COMSOL multiphysics version 3.5a was updated including the new experimental data following the same procedure of increasing conceptual model complexity as described in Weetjens *et al.* (2011, 2014). Parameter optimization was performed through coupling with the MATLAB Optimization Toolbox for HTO migration in the CP1 and Tribicarb-3D experiments. For the latter experiment, the optimization was done twice: (i) once only for the filters on the source piezometer R32-3 and the parallel piezometer R34-1, and (ii) using the experimental data from all three piezometers.

The main difference between the COMSOL and the MICOF model is that, instead of assuming a constant Darcy velocity $\overrightarrow{V_{Darcy}}$, the Darcy velocity (magnitude and direction) around the gallery is calculated by running a hydraulic calculation (Weetjens *et al.* 2014). Moreover, the filters are explicitly modelled as separate components.

Results

We start from the parameter values used for the blind predictions performed with the MICOF and COMSOL solutions, which are summarized in Table 2. These values are taken from Monsecour *et al.* (1990), Put *et al.* (1993), Aertsens *et al.* (2013) and Aertsens (2014) and, as already mentioned, are based on results from lab experiments at that time (Put and Henrion 1988; Put 1999; Henrion *et al.* 1991). More recent values, obtained from lab experiments performed after the values used for the blind predictions were fixed, can be found in Table 3. Clearly, these values do not fully correspond, as is the case for example for the accessible porosity η of $H^{14}CO_3^-$, and the recently obtained values from

lab experiments are not necessarily more accurate than the values used for the blind predictions. The differences are attributed to the different types of experiments used (e.g. Aertsens *et al.* 2008*a*, *b*) and the size of the datasets obtained for different samples which also shows the influence of local clay heterogeneities.

HTO

Because the dispersive term in the dispersion relation (3) is negligible, the experimental data are fitted by adjusting two parameters: the apparent diffusion coefficients $D_{app,x}$ ($=D_{app,y}$) and $D_{app,z}$. To avoid that the optimal values are dominated by the highest concentrations (at the source filter), the next function was minimized for the MICOF model:

$$\chi^2 = \sum_{i=1}^{N} \left(\frac{C_i - C_{exp,i}}{C_{exp,i}} \right)^2 \quad (7)$$

with N the number of measurements, $C_{exp,i}$ the experimentally measured concentration and C_i the fitted concentration according to expression (6). An alternative function used in the COMSOL optimizations is:

$$\chi^2 = \sum_{i=1}^{N} \left(\log_{10} \left(\frac{C_i}{C_{exp,i}} \right) \right)^2 \quad (8)$$

Table 3. *Summary of the fitted values for $D_{app,x}$ and $D_{app,z}$ from past and current modelling, compared to the values used for the original blind predictions and values obtained from lab experiments*

	$D_{app,x}$ (1×10^{-10} m^2 s^{-1})	$D_{app,z}$ (1×10^{-10} m^2 s^{-1})	AR (−)	η (−)	R^2
HTO					
Blind prediction	4.10	2.05		0.35	
CP1					
MICOF, Aertsens *et al.* (2013)	4.2	3.1	1.4	0.35	
	4.2	2.8	1.5	0.37	
COMSOL, Weetjens *et al.* (2014)	4.22 ± 0.03	2.50 ± 0.20	1.7	0.37	
MICOF, Present paper	4.25 ± 0.01	3.30 ± 0.15	1.3	0.35	0.9142
	4.25 ± 0.01	2.95 ± 0.15	1.4	0.37	0.9141
COMSOL, Present paper	4.09 ± 0.03	2.26 ± 0.15	1.8	0.35	0.9635
	4.10 ± 0.03	2.09 ± 0.13	2.0	0.37	0.9594
Tribicarb-3D					
MICOF, Aertsens *et al.* (2013)	5.0	2.0	2.5	0.35	
	5.0	2.0	2.5	0.37	
COMSOL, Aertsens *et al.* (2013)	5.1	2.1	2.4	0.37	
MICOF, Present paper	4.96 ± 0.01	2.07 ± 0.02	2.4	0.35	0.9552
	5.03 ± 0.01	2.09 ± 0.01	2.4	0.37	0.9599
COMSOL, Present paper, only $z \approx 0$	5.13 ± 0.03	2.70 ± 0.10	1.9	0.35	
	5.13 ± 0.03	2.42 ± 0.09	2.1	0.37	
COMSOL, Present paper, all data	4.99 ± 0.03	2.08 ± 0.02	2.4	0.35	0.9582
	5.05 ± 0.03	2.10 ± 0.02	2.4	0.37	0.9602
Laboratory experiments					
Aertsens *et al.* (1999)		2.3 ± 0.3		0.37	
Jacops *et al.* (2017)	7.3	4.1 ± 0.7	1.8		
$H^{14}CO_3^-$					
Blind prediction	1.2	0.6	2.0	0.33	
Tribicarb-3D					
MICOF, Aertsens *et al.* (2013)	1.0	0.7	1.4	0.33	
	1.0	1.1	0.9	0.26	
MICOF, Present paper	1.01 ± 0.01	0.99 ± 0.11	1.0	0.33	0.9949
	1.01 ± 0.01	1.59 ± 0.11	0.6	0.26	0.9948
Laboratory experiments					
Aertsens *et al.* (2008*b*)		0.6		0.26	

HTO fits of CP1 and Tribicarb-3D are performed with $\eta = 0.35$ (the value used in the blind predictions) and $\eta = 0.37$ (updated value based on Aertsens *et al.* 1999, and in line with best estimate value, Bruggeman *et al.* 2017). Similarly, for $H^{14}CO_3^-$ a value of $\eta = 0.33$ (blind predictions) and $\eta = 0.26$ (Aertsens *et al.* 2008*b*) is used. The anisotropy ratio (AR) is the ratio $D_{app,x}/D_{app,z}$. The coefficient of determination (R^2) indicates the goodness of fit. All uncertainties are 1σ.

The resulting fits for HTO (Fig. 4 for CP1 and Fig. 5 for Tribicarb-3D) are generally quite good with R^2 values higher than 0.9 (see Table 3). For CP1, the fitted concentrations systematically deviate from the experimental data for filter 2 (MICOF and COMSOL) and to a lesser extent for filter 3 (MICOF and COMSOL) and the source (injection) filter (COMSOL only). Due to advection, the predicted concentration difference in the $z = 0$ plane between filters at the same distance from the central filter (e.g. for CP1 filters 4 and 6, both at 1 m from the injection filter) increases with time and is larger for filter couples (for CP1: e.g. filters 4 and 6, filters 3 and 7) further away from the injection filter (Figs 4 & 5).

The optimal values for $D_{\text{app},x}$ (horizontal direction) (see Table 3) confirm the values obtained nearly ten years ago (Aertsens *et al.* 2013; Weetjens *et al.* 2014). For both *in situ* experiments, all fits lead to about the same value: $D_{\text{app},x} \approx 4.1$–$4.2 \times 10^{-10}$ m^2 s^{-1} for CP1 and $D_{\text{app},x} \approx 5 \times 10^{-10}$ m^2 s^{-1} for Tribicarb-3D. The reason for the difference between both values is unclear. This may be caused by local clay heterogeneities or a different disturbance due to the presence of the gallery.

For the remaining fit parameter, $D_{\text{app},z}$ (vertical direction), the situation is different. This parameter can only be determined accurately in case accurate measurements are available for positions z sufficiently far from the injection position $z = 0$. For CP1 (where for all filters $z = 0$), it has been shown (Weetjens *et al.* 2014) with COMSOL that assuming $D_{\text{app},z} = D_{\text{app},x}$ already leads to a good prediction of the experimental data. $D_{\text{app},x}$ is the dominating parameter and $D_{\text{app},z}$ only has a minor influence.

The dominance of $D_{\text{app},x}$ in CP1 is also clear by considering the fitted values for $D_{\text{app},z}$ and the corresponding uncertainties (all uncertainties in Table 3 are 1σ) in Table 3. Clearly, for CP1, where for all filters $z = 0$, the values of $D_{\text{app},z}$ obtained by MICOF and by COMSOL differ considerably: $D_{\text{app},z} \approx 3$ m^2 s^{-1} (MICOF) v. $D_{\text{app},z} \approx 2$ m^2 s^{-1} (COMSOL). Besides, the corresponding uncertainties ($\approx$ 0.1–0.3) are a factor ten higher than for $D_{\text{app},x}$ ($\approx$ 0.01–0.03), although $D_{\text{app},x}$ is larger than $D_{\text{app},z}$.

Similarly, there is also a difference in $D_{\text{app},z}$ values for COMSOL fits performed (i) considering all (Tribicarb-3D) data points and (ii) only the concentrations from filters on the source ($z = 0$) and the parallel piezometer ($z \approx 0$). For this second case ($z \approx 0$), the fits lead to $D_{\text{app},z}$ values significantly larger than the values used for the blind predictions (so obtained from lab experiments) with a high uncertainty (≈ 0.1, comparable with the uncertainties observed for CP1). In case all data are included in the fits (also those from the inclined piezometer), the optimal $D_{\text{app},z}$ values obtained by MICOF and COMSOL correspond ($D_{\text{app},z} \approx 2.1$ m^2 s^{-1}) and are in line with the value used by the blind prediction ($D_{\text{app},z} = 2.05$ m^2 s^{-1}) and lab-derived data (as most data are obtained for diffusion perpendicular to the bedding). At the same time, the uncertainty on $D_{\text{app},z}$ drops by about a factor of ten, to become comparable with the uncertainty on $D_{\text{app},x}$ ($\approx$ 0.01–0.03).

The uncertainties on $D_{\text{app},x}$ and $D_{\text{app},z}$ in Table 3 are obtained by fitting, assuming no errors on the values of the injected quantity Q_0, the accessible porosity η, the apparent velocity V_{app}, or the decay constant λ. It is, however, obvious that there will always be an error on these quantities. Changing the values of Q_0 or η changes $D_{\text{app},z}$ but hardly affects $D_{\text{app},x}$ (see Table 3). This is consistent with expression (6) which for $z = 0$ only depends on $D_{\text{app},z}$ by the factor $Q_0/\left(\eta\sqrt{D_{\text{app},z}}\right)$ (so e.g. a higher η does

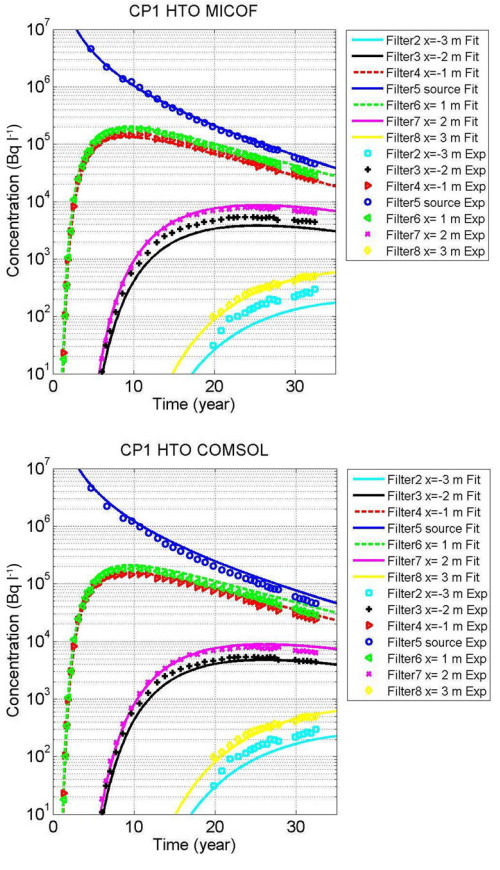

Fig. 4. Model predictions (lines) using the two modelling approaches (MICOF, COMSOL) v. measured HTO concentrations (symbols) for the CP1 *in situ* experiments for a fixed porosity $\eta = 0.37$ (optimal values for $D_{\text{app},x}$ and $D_{\text{app},z}$: see Table 3). For all filters, $y = z = 0$ and for the source $x = 0$.

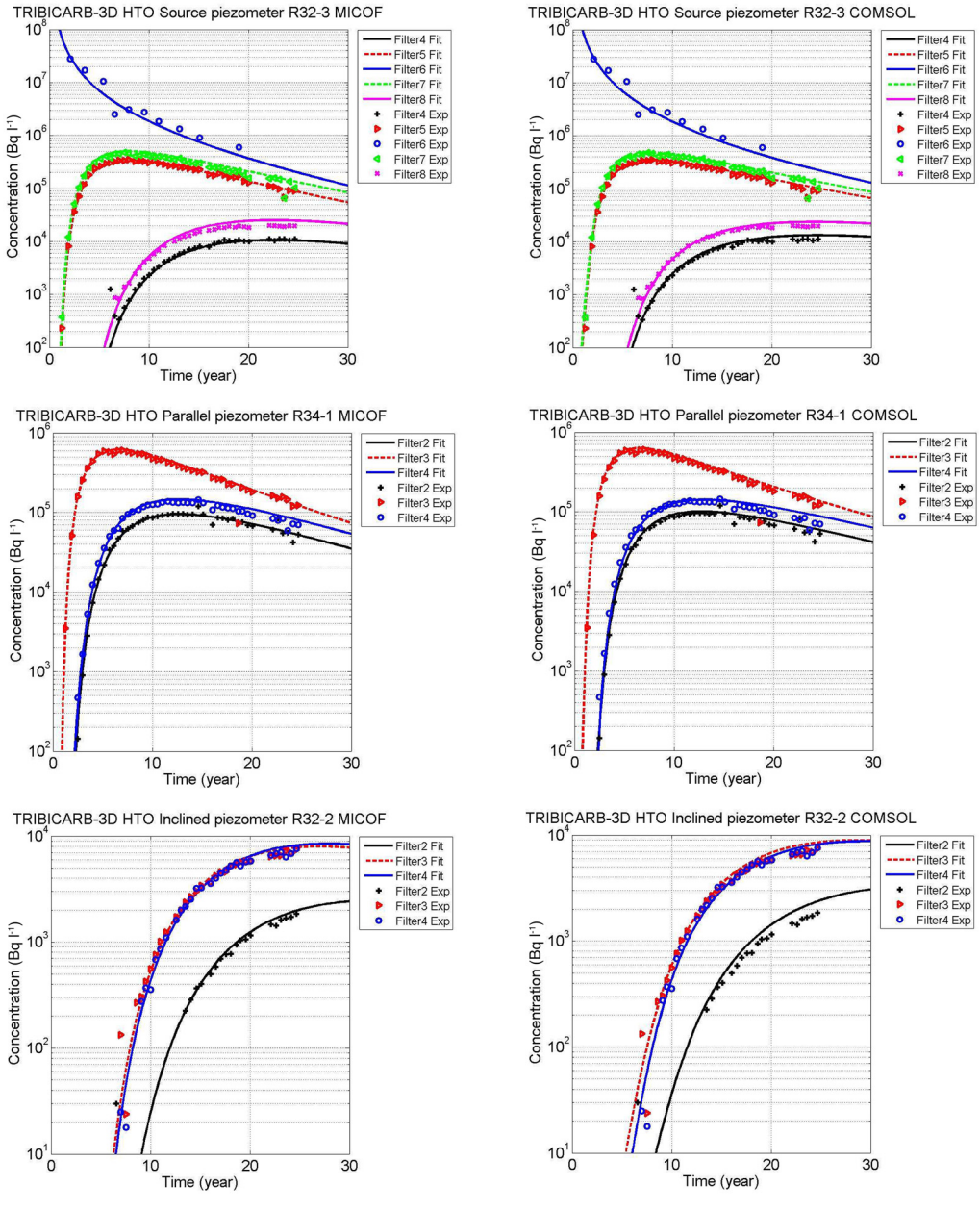

Fig. 5. Model predictions (lines) using the two modelling approaches (MICOF, COMSOL) v. measured HTO concentrations (symbols) for the Tribicarb-3D *in situ* experiments for a fixed porosity $\eta = 0.37$ (optimal values for $D_{\text{app},x}$ and $D_{\text{app},z}$: see Table 3).

not change $D_{\text{app},x}$ and corresponds to a lower $D_{\text{app},z}$ as observed for $z = 0$, e.g. CP1 and some Tribicarb-3D fits, in Table 3).

This is not the case for Tribicarb-3D due to the filters on the inclined piezometer: changing η hardly alters both $D_{\text{app},x}$ and $D_{\text{app},z}$ (Table 3) and the uncertainty on $D_{\text{app},z}$ is smaller than in CP1. Clearly, the uncertainties on the fitted parameters of Table 3 are correctly calculated and, as such, realistic. However, they are too small to be considered a general

uncertainty to be taken into account in, for example, safety assessments.

From the Tribicarb-3D results, the anisotropy ratio AR ($=D_{app,x}/D_{app,z}$) is approximately 2.4. Due to the high uncertainty on $D_{app,z}$, an accurate anisotropy ratio cannot be estimated from CP1.

Table 4 summarizes for HTO the apparent and effective diffusion coefficients D_{eff} ($D_{eff} = \eta D_{app}$), the accessible porosity and the anisotropy ratio for several clays studied for deep geological disposal. Of these clays, Boom Clay has the highest porosity, and correspondingly (due to Archie's law) the highest diffusion coefficients. Anisotropy, which strongly depends on the soil particle size (Hubert *et al.* 2013), is lower for Boom Clay than for the other clays of Table 4.

$H^{14}CO_3^-$

$H^{14}CO_3^-$-activity measurements were not always very reliable (as stated in the section 'the CP1 and Tribicarb-3D experiments'), resulting in more scatter on the experimental data (in particular at small times, see Fig. 6). For the inclined piezometer, no reliable data are available (Fig. 6), so that the fit is only done for filters with $z = 0$ or $z \approx 0$. This means that no accurate estimate for $D_{app,z}$ can be obtained. The agreement between the fitted concentrations with MICOF and the experimental data are quite good, with only a systematic deviation for filter 5 of the source piezometer R32-3 (see Fig. 6). Considering the good agreement between the $D_{app,x}$ values obtained by MICOF and COMSOL for CP1, it is expected that this is also the case for Tribicarb-3D. Therefore, no COMSOL fits have been performed for Tribicarb-3D.

The optimal value for $D_{app,x}$ (see Table 3) confirms the values obtained about ten years ago (Aertsens *et al.* 2013), differing about 20% from the value used for the blind prediction. Because for all filters $z \approx 0$, it is not surprising that the fitted $D_{app,z}$ values (Table 3) are unreliable and differ from the lab-derived data (which are only determined for cores taken perpendicular to the bedding plane). An accurate determination of $D_{app,z}$ requires reliable measurements on the filters of the inclined piezometer.

For the current timescales, the concentration $C(x, y, z, t)$ (expression (6)) is sensitive to the values of $D_{app,x}$, the injected quantity Q_0, and, in case of $z \neq 0$ measurement points (as in Tribicarb-3D for HTO) also to $D_{app,z}$. The concentration is rather insensitive to $V_{app,x}$. Therefore, it is not a problem to use expression (4) to determine the apparent velocity $V_{app,}$ although this expression is not correct for anions like $H^{14}CO_3^-$ (Aertsens *et al.* 2020). As a confirmation, both values of η ($\eta = 0.26$ and $\eta = 0.33$, Table 3) lead to a different apparent velocity $V_{app,}$ (estimated as V_{Darcy}/η by expression (4)) but the same $D_{app,x}$ (see Table 3). Also for HTO, $D_{app,x}$ is roughly independent of the η value (Table 3), and thus of the exact value of V_{app}.

Table 4. *Comparison of HTO apparent ($D_{app,x}$ and $D_{app,z}$) and effective ($D_{eff,x}$ and $D_{eff,z}$) diffusion coefficients, anisotropy ratio (AR) and accessible porosity (η) in several clays*

	$D_{app,x}$ (1×10^{-10} m^2 s^{-1})	$D_{eff,x}$ (1×10^{-10} m^2 s^{-1})	$D_{app,z}$ (1×10^{-10} m^2 s^{-1})	$D_{eff,z}$ (1×10^{-10} m^2 s^{-1})	AR (−)	η (−)
Boom Clay (Mol)						
Present study	4–5	1.4–1.9	2.1	0.7–0.8	2–2.4	0.35–0.37
Opalinus Clay (Mont Terri)						
Van Loon *et al.* (2004*a*)	3.2–3.6	0.54	0.8–1	0.14	3.9	0.14–0.17
Van Loon *et al.* (2004*b*)	2.7	0.4				0.15
Cormenzana *et al.* (2008), Wersin *et al.* (2005)	1.5–3.5	0.2–0.6	0.4–0.8	0.06–0.13	3–4	0.16
Leupin *et al.* (2017)		0.5–0.7			4–5	0.1–0.2
Toarcian Clay (Tournemire)						
Motellier *et al.* (2007)	1.8	0.21	0.6	0.075	2.8	0.12
Callovo-Oxfordian Clay (Bure)						
Cormenzana *et al.* (2008)	2–3	0.3–0.5	0.6–0.9	1.0–1.4	3.0	0.16
Descostes *et al.* (2008)			0.8–2.3	0.14–0.49		0.16–0.24

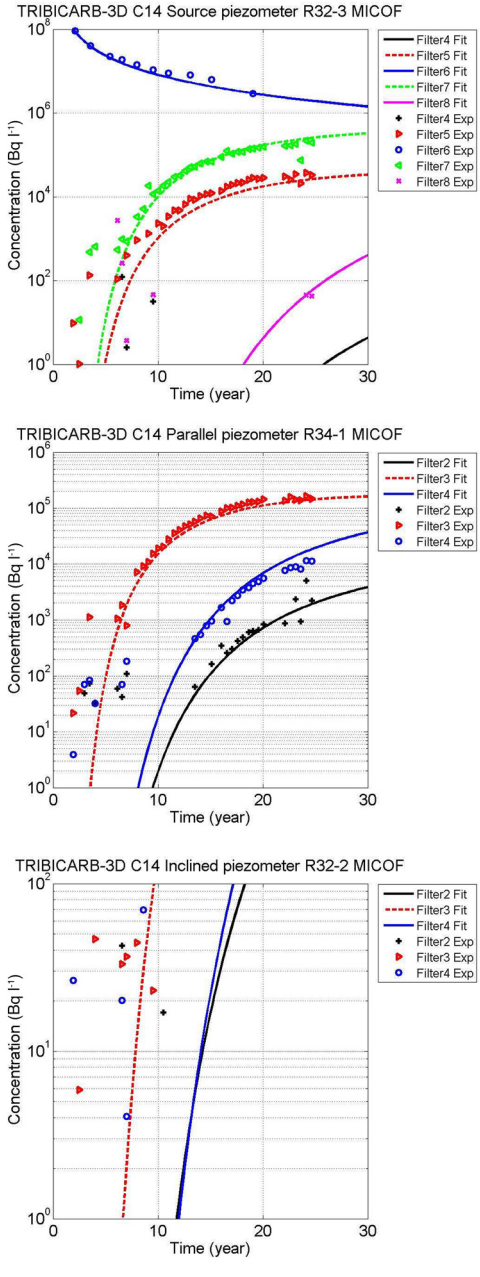

Fig. 6. Model predictions (lines) using the MICOF model v. measured $H^{14}CO_3^-$ concentrations (symbols) for the Tribicarb-3D *in situ* experiments for a fixed porosity $\eta = 0.26$ (optimal values for $D_{app,x}$ and $D_{app,z}$: see Table 3).

Conclusions

Compared to small-scale lab experiments where local heterogeneities can have important effects on the derived parameters, the long-term and large-scale *in situ* migration tests at the HADES URL provide high quality data over large distances and long times. This makes it possible to extract robust transport parameters that are relevant for *in situ* conditions complementing the data obtained from lab experiments. It is, however, important to note that for a single multi-filter piezometer (CP1) reliable data can only be obtained in the plane where the piezometer is installed (in this case direction parallel with the bedding plane). Only when a set of multi-filter piezometers is arranged in a 3D configuration (Tribicarb-3D), is it possible to obtain reliable transport parameters parallel with and perpendicular to the bedding.

In terms of upscaling, these *in situ* diffusion tests (CP1 and Tribicarb-3D) validate the models based on the classic dispersion–advection equation and associated parameters. It turned out that the analytical and numerical models perform equally well and that the parameters obtained on a small-scale (lab) can be applied on a larger scale. The experiments continue to provide data that enable reliable parameter estimation. This all provides confidence that the migration of HTO and $H^{14}CO_3^-$ is correctly understood at the metre scale.

Acknowledgements This paper benefited considerably from the constructive remarks of two anonymous referees.

Competing interest The authors declare that they have no known competing financial interests or personal relationships that could have appeared to influence the work reported in this paper.

Author contributions **MA**: writing – original draft (lead), writing – review & editing (lead); **EW**: writing – original draft (equal), writing – review & editing (equal); **JG**: writing – original draft (equal), writing – review & editing (equal); **NM**: writing – original draft (equal), writing – review & editing (equal); **SB**: writing – original draft (supporting), writing – review & editing (supporting).

Funding This research received no specific grant from any funding agency in the public, commercial, or not-for-profit sectors.

Data availability All data generated or analysed during this study are included in this published article

References

Aertsens, M. 2014. *Overview of migration experiments in the HADES Underground Research Facility at Mol*. SCK CEN report ER-164. Mol, Belgium.

Aertsens, M., Put, M. and Dierckx, A. 1999. An analytical model for pulse experiments. *Proceedings of Modelling*

of transport processes in soils at various scales in time and space, 24–26 November 1999, Leuven, Belgium, 67–76.

Aertsens, M., Put, M. and Dierckx, A. 2003. An analytical model for the interpretation of pulse injection experiments performed for testing the spatial variability of clay formations. *Journal of Contaminant Hydrology*, **61**, 423–436, https://doi.org/10.1016/S0169-7722(02)00118-3

Aertsens, M., Wemaere, I. and Wouters, L. 2004. Spatial variability of transport parameters in the Boom Clay. *Applied Clay Science*, **26**, 37–45, https://doi.org/10.1016/j.clay.2003.09.015

Aertsens, M., De Cannière, P., Lemmens, K., Maes, N. and Moors, H. 2008*a*. Overview and consistency of migration experiments in clay. *Physics and Chemistry of the Earth*, **33**, 1019–1025, https://doi.org/10.1016/j.pce.2008.05.019

Aertsens, M., Van Gompel, M., De Cannière, P., Maes, N. and Dierckx, A. 2008*b*. Vertical distribution of HCO_3-transport parameters in Boom Clay in the Mol-1 borehole (Mol, Belgium). *Physics and Chemistry of the Earth*, **33**, S61–S66, https://doi.org/10.1016/j.pce.2008.10.060

Aertsens, M., Maes, N. and Van Ravestyn, L. 2013. Overview of radionuclide migration experiments in the HADES Underground Research Facility at Mol (Belgium). *Clay Minerals*, **48**, 153–166, https://doi.org/10.1180/claymin.2013.048.2.01

Aertsens, M., Maes, N., Govaerts, J. and Durce, D. 2020. Why tracer migration experiments with a pressure gradient do not always allow a correct estimation of the accessible porosity in clays. *Applied Geochemistry*, **120**, 104672, https://doi.org/10.1016/j.apgeochem.2020.104672

Altmann, S., Aertsens, M. *et al*. 2015. *Processes of cation migration in clayrocks*. Final scientific report of the Catclay European project. Report CEA-R 6410.

Baetsle, L. 1998. Disposal of conditioned HLW matrices and interaction with a deep clay layer as host formation. *In*: Stenhouse, M. and Kirko, V. (eds) *Defence Nuclear Waste Disposal in Russia: international perspective*. Kluwer Academic, Netherlands, 33–43.

Bastiaens, W., Bernier, F. and Li, X.L. 2007. Experiments and conclusions on fracturing, self-healing and self-sealing processes in clays. *Physics and Chemistry of the Earth*, **32**, 600–615, https://doi.org/10.1016/j.pce.2006.04.026

Beaufays, R., Blommaert, W. *et al*. 1994. *Nuclear Science and Technology: characterization of the Boom Clay and its multilayered hydrogeological environment*. Report EUR-14961, European Commission (contract FI1 W/0055).

Bruggeman, C. and Maes, N. 2017. *Radionuclide migration and retention in Boom Clay*. SCK CEN report ER-0345. Mol, Belgium.

Bruggeman, C., Maes, N., Aertsens, M. and Salah, S. 2017. Tritiated water retention and migration behaviour in Boom Clay: topical report – status 2015. SCKCEN Reports, ER-0408, Mol, Belgium.

Chen, Y., Glaus, M., Van Loon, L. and Mäder, U. 2018*a*. Transport of low molecular weight organic compounds in compacted illite and kaolinite. *Chemosphere*, **198**, 226–237, https://doi.org/10.1016/j.chemosphere.2018.01.137

Chen, Y., Glaus, M., Van Loon, L. and Mäder, U. 2018*b*. Transport behavior of low molecular organic compounds in multimineral clay systems. A comparison between measured and predicted values. *Applied Clay Science*, **165**, 247–256, https://doi.org/10.1016/j.clay.2018.08.004

Cormenzana, J.L., Garcia-Gutiérrez, M., Missana, T. and Alonso, U. 2008. Modelling large-scale laboratory HTO and strontium diffusion experiments in Monte Terri and Bure clay rocks. *Physics and Chemistry of the Earth*, **33**, 949–956, https://doi.org/10.1016/j.pce.2008.05.006

De Cannière, P., Moors, H., Lolivier, P., De Preter, P. and Put, M. 1996. *Nuclear Science and Technology: laboratory and in situ migration experiments in the Boom Clay*. Report EUR-16927, European Commission.

De Cannière, P., Volckaert, G., Ortiz, L., Put, M., Sneyers, A. and Neerdael, B. 2007. Transport of solutes and gas in soft clay: Experience from the HADES URL – Mont Terri Project. *Proceedings of the 10-Year Anniversary Workshop, Report*. Swiss Geological Survey, 2, 61–64.

De Craen, M. 1998. *The origin of septarian carbonate concretions in organic-rich argillaceous sediments*. PhD thesis, KU Leuven, Belgium.

De Craen, M. 2006. The Boom Clay geochemistry: Natural evidence. *Materials Research Society Symposium Proceedings*, **932**, https://doi.org/10.1557/PROC-932-5.1

De Craen, M., Wang, L., Van Geet, M. and Moors, H. 2004. *Geochemistry of Boom Clay pore water at the Mol site - status 2004*. SCK CEN Report BLG-990. Mol, Belgium.

Delay, J., Bossart, P. *et al*. 2014. Three decades of underground research laboratories: what have we learned? *Geological Society, London, Special Publications*, **400**, 7–32, https://doi.org/10.1144/SP400.1

De Preter, P., Put, M.J., De Canniere, P. and Moors, H. 1992. *Migration of radionuclides in Boom Clay*. State-of-the-Art report June 1992, NIROND 92-07, Contract FI 2W/0039. ONDRAF/NIRAS, Brussels, Belgium.

Descostes, M., Blin, V. *et al*. 2008. Diffusion of anionic species in Callovo-Oxfordian argillites and Oxfordian limestones (Meuse/Haute-Marne, France). *Applied Geochemistry*, **23**, 655–677, https://doi.org/10.1016/j.apgeochem.2007.11.003

Dierckx, A., Put, M. *et al*. 2000. *Nuclear Science and Technology: Transport of Radionuclides due to Complexaton with Organic Matter in Clay formations – Trancom-Clay*. Report EUR 19135, European Commission.

Durce, D., Bruggeman, C., Maes, N., Van Ravestyn, L. and Brabants, G. 2015. Partitioning of organic matter in Boom Clay: leachable v. mobile organic matter. *Applied Geochemistry*, **63**, 169–181, https://doi.org/10.1016/j.apgeochem.2015.08.009

Frederickx, L. 2019. *An advanced mineralogical study of the clay mineral fractions in the Boom Clay*. PhD thesis, KU Leuven, Belgium.

Frederickx, L., Honty, M., De Craen, M. and Elsen, J. 2021. Evaluating the quantification of the clay mineralogy of the Rupelian Boom Clay in Belgium by a detailed study

of the size fractions. *Applied Clay Science*, **201**, 105954, https://doi.org/10.1016/j.clay.2020.105954

Govaerts, J., Maes, N., Durce, D., Aertsens, M. and Brassinnes, S. 2022. Coupled flow and transport modelling of a large-scale *in situ* migration experiment with ^{14}C-labelled natural organic matter colloids in Boom Clay. *Geological Society, London, Special Publications*, **536**, https://doi.org/10.1144/SP536-2022-22

Henrion, P., Put, J. and Van Gompel, M. 1991. The influence of compaction on the diffusion of non-sorbed species in Boom Clay. *Radioactive Waste Management and the Nuclear Fuel Cycle*, **16**, 1–14.

Hubert, F., Bihannic, I. *et al*. 2013. Investigating the anisotropic features of particle orientation in synthetic swelling clay porous media. *Clays and Clay Minerals*, **61**, 397–415, https://doi.org/10.1346/CCMN.2013.0610501

Hunt, A. and Sahimi, M. 2017. Flow, transport, and reaction in porous media: percolation scaling, critical-path analysis and effective medium approximation. *Review of Geophysics*, **55**, 993–1078, https://doi.org/10.1002/2017RG000558

Hunt, A., Skinner, T., Ewing, P. and Ghanbarian-Alavijeh, B. 2011. Dispersion of solutes in porous media. *European Physical Journal B*, **80**, 411–432, https://doi.org/10.1140/epjb/e2011-10805-y

Jacops, E., Aertsens, M. *et al*. 2017. Interplay of molecular size and pore network geometry on the diffusion of dissolved gasses and HTO in Boom Clay. *Applied Geochemistry*, **76**, 182–195, https://doi.org/10.1016/j.apgeochem.2016.11.022

Leupin, O., Van Loon, L., Gimmi, T., Wersin, P. and Soler, J. 2017. Exploring diffusion and sorption processes at the Mont Terri rock laboratory (Switzerland): lessons learned from 20 years of field research. *Swiss Journal of Geosciences*, **110**, 391–403, https://doi.org/10.1007/s00015-016-0254-z

Maes, N., Bruggeman, C., Govaerts, J., Martens, E., Salah, S. and Van Gompel, M. 2011. A consistent phenomenological model for natural organic matter linked migration of Tc(IV), Cm(III), Np(IV), Pu(III/IV) and Pa(V) in the Boom Clay. *Physics and Chemistry of the Earth*, **36**, 1590–1599, https://doi.org/10.1016/j.pce.2011.10.003

Marivoet, J. 1988. *PAGIS: Performance assessment of geological isolation systems for radioactive waste disposal in clay formations*. Report EUR-11775, European Commission and SCK CEN Report R-2748. Mol, Belgium.

Marivoet, J. and Weetjens, E. 2007. The importance of mobile fission products for long-term safety in the case of disposal of vitrified high-level waste and spent fuel in a clay formation. *Proceedings of Mobile fission and activation products in nuclear waste disposal*, 16–19 January 2007, La Baule, France, OECD/NEA, Issu-les-Moulineaux, France.

Marivoet, J. and Zeevaert, T. 1991. *PACOMA: Performance assessment of the geological disposal of medium level and alpha waste in a clay formation in Belgium*. Report EUR-13042, European Commission.

Martens, E., Maes, N., Weetjens, E., Van Gompel, M. and Van Ravestyn, L. 2010. Modelling of a large-scale in-situ migration experiment with 14C-labelled natural organic matter in Boom Clay. *Radiochimica Acta*, **98**, 695–701, https://doi.org/10.1524/RACT.2010.1770

Mazurek, M., Alt-Epping, P. *et al*. 2011. Natural tracer profiles across argillaceous formations. *Applied Geochemistry*, **26**, 1035–1064, https://doi.org/10.1016/J.apgeochem.2011.03.124

Monsecour, M., Put, M., Fonteyne, A. and Yoshida, H. 1990. Migration experiments in the underground facility at Mol to validate safety assessment model. *Geoval, Symposium on validation of geosphere flow and transport models*, 14–17 May 1990, Stockholm, OECD.

Motellier, S., Devol-Brown, I., Savoye, S., Thoby, D. and Alberto, J.-C. 2007. Evaluation of tritiated water diffusion through the Toarcian clayey formation of the Tournemire experimental site (France). *Journal of Contaminant Hydrology*, **94**, 99–108, https://doi.org/10.1016/j.jconhyd.2007.05.012

Put, M. 1992. *Three dimensional in situ migration experiment in the Boom Clay formation at the Mol site in Belgium. INTRAVAL phase 2 Test case description and data*. Report NIROND 92-07. ONDRAF/NIRAS, Brussels, Belgium.

Put, M. 1999. *Geological disposal of conditioned high-level and long-lived radioactive waste – Tasks 2.1 to 4.6 & Operation and maintenance of the URF, Progress report to NIRAS/ONDRAF for the first semester of 1998*. Report R-3380, October 1999. SCK CEN, Mol, Belgium.

Put, M. and Henrion, P. 1988. An improved method to evaluate radionuclide migration model parameters from flow-through diffusion tests in reconsolidated clay plugs. *Radiochimica Acta*, **44/45**, 343–347, https://doi.org/10.1524/ract.1988.4445.2.343

Put, M. and Henrion, P. 1992. *Nuclear Science and Technology: Modelling of radionuclide migration and heat transport from an HLW repository in Boom Clay*. Report EUR-14156, European Commission (contract FI1 W/0055).

Put, M., Monsecour, M., Fonteyne, A. and Yoshida, H. 1991. Estimation of the migration parameters for the Boom Clay formation by percolation experiments on undisturbed clay cores. *Materials Research Society Symposium Proceedings*, **212**, 823–829, https://doi.org/10.1557/PROC-212-823

Put, M., De Cannière, P., Moors, H., Fonteyne, A. and De Preter, P. 1993. Validation of performance assessment model by large-scale in situ migration experiments. *Proceedings of an international symposium on geological disposal of spent fuel, high level and alpha bearing wastes jointly organized by the International Atomic Energy Agency, the Commission of the European Communities and the OECD Nuclear Energy Agency*, 19–23 October 1992, Antwerp. IAEA, Vienna, 319–326.

Salah, S., Bruggeman, C., Maes, N., Liu, D., Wang, L. and Van Iseghem, P. 2013. Radionuclide behaviour and geochemistry in Boom Clay within the framework of geological disposal of High-level waste. *Ceramic transaction*, **241**, 113–125, https://doi.org/10.1002/9781118751176.ch11

Vandenberghe, N. 1978. *Sedimentology of the Boom Clay (Rupelian) in Belgium*. Verhandeling Koninklijke Academie voor Wetenschappen, Letteren en Schone Kunsten van België, Klasse Wetenschappen **XL**. Belgium.

Van Loon, L., Soler, J., Müller, W. and Bradbury, M. 2004*a*. Anisotropic diffusion in layered argillaceous rocks: a case study with Opalinus Clay. *Environmental Science and Technology*, **38**, 5721–25728, https://doi.org/10.1021/es049937g

Van Loon, L., Wersin, P., Soler, J., Eikenberg, J., Gimmi, T., Hernan, P., Dewonck, S. and Savoye, S. 2004*b*. In-situ diffusion of HTO, $^{22}Na^{+}$, Cs^{+} and I^{-} in Opalinus Clay at the Mont Terri underground rock laboratory. *Radiochimica Acta*, **92**, 757–763, https://doi.org/10.1524/ract.92.9.757.54988

Weetjens, E., Govaerts, J. and Aertsens, M. 2011. *Model and parameter validation based on in situ experiments in Boom Clay*. SCK CEN-report ER-171. Mol, Belgium.

Weetjens, E., Maes, N. and Van Ravestyn, L. 2014. Model validation based on in situ radionuclide migration tests in Boom Clay: status of large-scale migration experiments, 24 years after injection. *Geological Society, London, Special Publications*, **400**, 613–623, https://doi.org/10.1144/SP400.39

Wersin, P., Dewonck, S. *et al*. 2005. Diffusion of HTO, iodine, sodium-22 and caesium in Opalinus Clay: a combined field, laboratory and modelling study. *International Meeting Clays in Natural & Engineered Barriers for Radioactive Waste Confinement*, March 14–18, Tours, France.

Yu, L., Rogiers, B., Gedeon, M., Marivoet, J., De Craen, M. and Mallants, D. 2013. A critical review of laboratory and in-situ hydraulic conductivity measurements for the Boom Clay in Belgium. *Applied Clay Science*, **75–76**, 1–12, https://doi.org/10.1016/j.clay.2013.02.018

Zeelmaekers, E., Honty, M. *et al*. 2015. Qualitative and quantitative mineralogical composition of the Rupelian Boom Clay in Belgium. *Clay Minerals*, **50**, 249–272, https://doi.org/10.1180/claymin.2015.050.2.08